Controllability of Structural Brain Networks and the Waxing and Waning of Negative Affect in Daily Life

Supplement 1

Supplemental Methods

Anatomical data preprocessing. The T1-weighted (T1w) image was corrected for intensity non-uniformity (INU) using N4BiasFieldCorrection (1), and used as T1w-reference throughout the workflow. The T1w-reference was then skull-stripped using antsBrainExtraction.sh (ANTs 2.3.1), using OASIS as the target template. Spatial normalization to the ICBM 152 Nonlinear Asymmetrical template version 2009c (2) was performed through nonlinear registration with antsRegistration (ANTs 2.3.1, RRID:SCR_004757)(3), using brain-extracted versions of both T1w volume and template. Brain tissue segmentation of cerebrospinal fluid (CSF), white-matter (WM) and gray-matter (GM) was performed on the brain-extracted T1w using FAST (FSL 6.0.3:b862cdd5, RRID:SCR_002823) (4).

Diffusion data preprocessing. MP-PCA denoising as implemented in MRtrix3's dwidenoise (5) was applied with a 5- voxel window. After MP-PCA, Gibbs unringing was performed using MRtrix3's mrdegibbs (6). Following unringing, B1 field inhomogeneity was corrected using dwibiascorrect from MRtrix3 with the N4 algorithm (1). After B1 bias correction, the mean intensity of the DWI series was adjusted so all the mean intensity of the b=0 images matched across each separate DWI scanning sequence. FSL (version 6.0.3:b862cdd5)'s eddy was used for head motion correction and Eddy current correction (7). Eddy was configured with a q-space smoothing factor of 10, a total of 5 iterations, and 1000 voxels used to estimate hyperparameters. A linear first level model and a linear second level model were used to characterize Eddy current-related spatial distortion. q-space coordinates were forcefully assigned to shells. Field offset was attempted to be separated from subject movement. Shells were aligned post-eddy. Eddy's outlier replacement was run (7). Data were grouped by slice, only including values from slices determined to contain at least 250 intracerebral voxels. Groups deviating by more than 4 standard deviations from the prediction had their data replaced with imputed values. Fieldmaps were collected with reversed phase-encode blips, resulting in pairs of images with distortions going in opposite directions. Here, a b=0 fieldmap image with reversed phase encoding direction was used along with b=0 images extracted from the DWI scans. From these pairs, the susceptibility-induced off-resonance field was estimated using a method similar to that described in(8). The fieldmaps were ultimately incorporated into the Eddy current and head motion correction interpolation. Final interpolation was performed using the jac method.

Several confounding time-series were calculated based on the preprocessed DWI: framewise displacement (FD) using the implementation in Nipype (following the definitions by Power et al., 2014). The head-motion estimates calculated in the correction step were also placed within the corresponding confounds file. Slicewise cross correlation was also calculated. The DWI time-series were resampled to ACPC, generating a preprocessed DWI run in ACPC space with 1.7 mm isotropic voxels. Many internal operations of QSIPrep use Nilearn 0.7.0 (Abraham et al., 2014; RRID:SCR_001362) and Dipy (11).

Supplemental Analyses

Specificity to Average Controllability

To examine the extent to which our analyses were specific to average controllability, we included analyses using other network measures: i) strength, ii) clustering coefficient, iii) betweenness centrality, and iv) closeness centrality. Briefly, strength represents a region's direct connections to the rest of the brain. Strength for each region is calculated by summing the edge weights over all regions in the network (12). The clustering coefficient of a region measures the possibility that any two neighbors of the node are also connected (13). Betweenness centrality represents the fraction of all shortest paths in a network that contain a given node, with high values indicating the region participates in a large number of shortest paths (14). Closeness centrality represents how close a region is to other regions and is calculated as the average of the shortest path from the node to every other node in the network (15).

Strength

We found no association between average negative affect (p's ≥ 0.06, p_{FDR}'s ≥ 0.53). or negative affect variability (p's ≥ 0.04, p_{FDR}'s ≥ 0.48) and strength across the 17 subsystems following false discovery rate control.

Clustering Coefficient

We found no association between average negative affect (p's ≥ 0.05, p_{FDR}'s ≥ 0.42) or negative affect variability (p's ≥ 0.40, p_{FDR}'s ≥ 0.98) and clustering coefficient across the 17 subsystems following false discovery rate control.

Betweenness Centrality

We found no association between average negative affect (p's ≥ 0.15, p_{FDR}'s ≥ 0.93) or negative affect variability (p's ≥ 0.07, p_{FDR}'s ≥ 0.74) and betweenness centrality across the 17 subsystems following false discovery rate control.

Closeness Centrality

We found no association between average negative affect (p's ≥ 0.04, p_{FDR}'s ≥ 0.10) or negative affect variability (p's ≥ 0.71, p_{FDR}'s ≥ 0.99) and closeness centrality across the 17 subsystems following false discovery rate control.

Specificity to Negative Affect Variability

To examine the extent to which our analyses were specific to negative affect variability (intraindividual standard deviation), we included analyses using other measures of affect dynamics: i) negative affect instability and ii) negative affect inertia. Negative affect instability was measured using the mean successive square difference (MSSD) of negative affect (16–19), which provides an index of the moment-to-moment fluctuations in negative affect. Higher values MSSD values indicate increased emotional instability. Negative affect inertia was measured using negative affect autocorrelation computed with a lag of one (16,19,20), providing an index of the extent to which negative affect at time t was correlated with negative affect at time t+1. Higher negative affect inertia values suggest resistance to change (i.e., high temporal dependency) whereas low scores suggest low temporal dependency. Negative affect variability and negative affect instability were strongly and positively correlated ($r = 0.81$, $p < 0.001$ [95%

CI: 0.73 to 0.87]; see Supplemental Table S10). However, negative affect inertia was not significantly correlated with either negative affect variability or negative affect instability (r's ≤ 0.17, p's ≥ 0.10 [95% CI: -0.03 to 0.36]; see Supplemental Table S10).

Negative Affect Instability

We found no association between negative affect instability and average controllability of the cingulo-insular system following false discovery rate control (b = 420.76, p = 0.03, p_{FDR} = 0.06; see Supplemental Table S7).

Negative Affect Inertia

We found no association between negative affect inertia and average controllability of the cingulo-insular system following false discovery rate control (b = 0.18, p = 0.21, p_{FDR} = 0.64; see Supplemental Table S8).

Supplemental Table S1. Correlations and descriptive statistics of key study variables.

Variable	*M*	*SD*	1	2	3	4	5
1. Average controllability	-0.01	0.18					
2. Negative affect	37.38	14.29	.12				
3. Negative affect variability	17.88	6.44	.29**	.32**			
4. CESD	9.78	5.00	.18	.42**	.30**		
5. Brain volume	1586117.36	155450.31	.26*	.01	.05	.13	
6. In-scanner motion	5068.38	2991.58	.10	.02	.01	-.28**	.12

Note. M and *SD* are used to represent mean and standard deviation, respectively. * indicates $p < 0.05$, ** indicates $p < 0.01$. CESD = Center for Epidemiological Studies Depression scale. $N = 95$.

Supplemental Table S2. Nodes included in the cingulo-insular (Salience Ventral Attention A) system.

Node Label	X, Y, Z Coordinates	Component Name
LH_SalVentAttnA_FrMed_1	(-6,9,41)	Frontal medial
LH_SalVentAttnA_FrMed_2	(-6,-3,65)	
RH_SalVentAttnA_FrMed_1	(7,9,41)	
RH_SalVentAttnA_FrMed_2	(8,3,66)	
LH_SalVentAttnA_FrOper_1	(-39,1,11)	Frontal operculum
LH_SalVentAttnA_FrOper_2	(-51,9,11)	
RH_SalVentAttnA_FrOper_1	(43,7,4)	
LH_SalVentAttnA_Ins_1	(-39,-4,-4)	Insula
RH_SalVentAttnA_Ins_1	(41,6,-15)	
RH_SalVentAttnA_Ins_2	(46,-4,-4)	
LH_SalVentAttnA_ParMed_1	(-11,-35,46)	Parietal medial
RH_SalVentAttnA_ParMed_1	(10,-15,41)	
RH_SalVentAttnA_ParMed_2	(11,-36,47)	
LH_SalVentAttnA_ParOper_1	(-61,-26,28)	Parietal operculum
RH_SalVentAttnA_ParOper_1	(60,-26,27)	
RH_SalVentAttnA_PrC_1	(51,4,40)	Precentral

Note. LH = left hemisphere, RH = right hemisphere.

Supplemental Table S3. Associations with Neurosynth meta-analysis of cingulo-insular (Salience Ventral Attention A) system coordinates

Coordinates	Top 10 Entries
(-6,9,41)	Motor; supplementary; supplementary motor; anterior cingulate; task; cingulate; anterior insula; primary motor; autonomic; anterior
(-6,-3,65)	Motor; movements; supplementary; supplementary motor; tapping; premotor; finger; imagery; motor cortex; primary motor
(7,9,41)	Motor; supplementary; supplementary motor; anterior cingulate; task; cingulate; anterior insula; primary motor; autonomic; anterior
(8,3,66)	Motor; supplementary; supplementary motor; movements; movement; eye fields; saccade; reorganization; foor; primary motor
(-39,1,11)	Insula; pain; electrical; secondary somatosensory; muscle; somatosensory; painful; somatosensory cortex; autonomic; primary somatosensory
(-51,9,11)	Phonological; inferior frontal; language; broca; inferior; execution; premotor; frontal; word; frontal gyrus
(43,7,4)	Insula; pain; anterior insula; thalamus; painful; anterior cingulate; sensation; insular; insula anterior; posterior insula
(-39,-4,-4)	Insula; pain; posterior insula; insular; insular cortex' amygdala anterior; empathy; anterior insula; events; painful
(41,6,-15)	Insula; taste; insular; amygdala; insular cortex; skin conductance; conductance; amygdala anterior; anterior; eating
(46,-4,-4)	Insula; musical; insular cortex; secondary somatosensory; listening; insula anterior; anterior insula; empathy; insular; putamen
(-11,-35,46)	Insula anterior; middle cingulate; anterior insula; recollection; autonomic; abilities; ability; abstract; abuse; acc
(10,-15,41)	Anterior insula; social; theory mind; abilities; ability; abstract; abuse; acc; accumbens; accurate
(11,-36,47)	Precuneus; social; hubs; middle cingulate; pain; asd; abilities; ability; abstract; abuse
(-61,-26,28)	Somatosensory; somatosensory cortex; supramarginal; pain; primary somatosensory; somatosensory cortices; supramarginal gyrus; tactile; motor; touch
(60,-26,27)	Somatosensory; pain; somatosensory cortices; sensorimotor; secondary somatosensory; somatosensory cortex; ipsilateral; motor; supplementary motor; supplementary
(51,4,40)	Premotor; frontal eye; eye; motor; premotor cortex; movements; eye field; eye movements; ventral premotor; pre sma

Supplemental Table S4. Results of the multilevel model examining associations between average controllability of the cingulo-insular network with negative affect variability.

Effect	Estimate	Standard error	*p*	*d*	Confidence interval	
					Lower	Upper
Negative Affect Variability						
Fixed effects						
Intercept	13.12***	1.75	< 0.001		9.63	16.61
Average controllability	9.57**	3.70	0.01	0.57	2.19	16.94
Negative Affect	0.13**	0.04	0.004	0.65	0.04	0.22
Total brain volume	-0.12	0.64	0.85	-0.04	-1.40	1.15
In-scanner motion	-0.13	0.63	0.83	-0.05	-1.38	1.11
Random effects						
Intercept	0.08					
Residual	36.13					

Note. 95 participants nested in 10 groups; ***$p < 0.001$; **$p \leq 0.01$. Total brain volume and in-scanner motion were sample-mean centered; average controllability was rank-based inverse normal transformed.

Supplemental Table S5. Results of the multilevel model examining associations between average controllability of the cingulo-insular system with negative affect variability controlling for depressive symptoms.

Effect	Estimate	Standard error	*p*	*d*	Confidence interval	
					Lower	Upper
Negative Affect Variability						
Fixed effects						
Intercept	11.85***	1.91	< 0.001		8.06	15.65
Average controllability	8.42**	3.82	0.03	0.50	0.82	16.02
Negative Affect	0.10**	0.05	0.05	0.46	0	0.19
CESD	0.25	0.15	0.11	0.37	-0.05	0.55
Total brain volume	-0.52	0.67	0.44	-0.18	-1.86	0.82
In-scanner motion	0.31	0.69	0.66	0.10	-1.07	1.68
Random effects						
Intercept	0.27					
Residual	35.92					

Note. 95 participants nested in 10 groups; ***$p < 0.001$; **$p \leq 0.01$. CESD = sum scores on Center for Epidemiologic Studies-Depression Scale. Total brain volume and in-scanner motion were sample-mean centered; average controllability was rank-based inverse normal transformed.

Supplemental Table S6. Results of the multilevel models examining associations between average controllability of the remaining 16 brain networks with negative affect variability.

Effect	Estimate	Standard error	*p*	p_{FDR}	*d*	Confidence interval Lower	Confidence interval Upper
Control A							
Fixed effects							
Intercept	13.04***	1.82	< 0.001	< 0.001		9.41	16.67
Average controllability	2.62	2.02	0.20	0.47	0.29	-1.40	6.65
Negative Affect	0.13**	0.05	0.005	0.01	0.66	0.04	0.22
Total brain volume	0.006	0.67	0.99	0.99	0.002	-1.32	1.33
In-scanner motion	-0.10	0.68	0.88	0.99	-0.03	-1.46	1.25
Random effects							
Intercept	0.57						
Residual	37.68						
Control B							
Fixed effects							
Intercept	12.82***	1.82	< 0.001	< 0.001		9.20	16.46
Average controllability	1.11	1.46	0.45	0.85	0.17	-1.79	4.01
Negative Affect	0.14**	0.04	0.003	0.009	0.68	0.05	0.23
Total brain volume	0.07	0.69	0.92	0.99	0.02	-1.31	1.44
In-scanner motion	-0.06	0.70	0.93	0.99	-0.01	-1.45	1.33
Random effects							
Intercept	0.83						
Residual	37.97						
Control C							
Fixed effects							
Intercept	12.54***	1.82	< 0.001	< 0.001		8.91	16.17
Average controllability	1.43	1.65	0.39	0.77	0.19	-1.86	4.72
Negative Affect	0.14**	0.04	0.002	0.008	0.71	0.05	0.23
Total brain volume	0.24	0.64	0.70	0.99	0.09	-1.03	1.52
In-scanner motion	-0.18	0.72	0.81	0.99	-0.06	-1.61	1.26
Random effects							
Intercept	0.88						
Residual	37.87						
Default A							
Fixed effects							
Intercept	12.83	1.81	< 0.001	< 0.001		9.23	16.42
Average controllability	2.37	1.96	0.23	0.53	0.27	-1.53	6.26
Negative Affect	0.14	0.04	0.003	0.008	0.68	0.05	0.23
Total brain volume	-0.08	0.70	0.91	0.99	-0.02	-1.46	1.31
In-scanner motion	-0.28	0.70	0.69	0.99	-0.09	-1.68	1.12
Random effects							
Intercept	0.50						
Residual	37.83						
Default B							
Fixed effects							
Intercept	12.72***	1.80	< 0.001	< 0.001		9.14	16.32
Average controllability	1.52	1.33	0.26	0.59	0.25	-1.14	4.17
Negative Affect	0.14**	0.04	0.003	0.008	0.69	0.05	0.23
Total brain volume	-0.02	0.69	0.98	0.99	-0.006	-1.38	1.34
In-scanner motion	-0.13	0.68	0.84	0.99	-0.04	-1.50	1.23

Random effects							
Intercept	0.56						
Residual	37.85						
Default C							
Fixed effects							
Intercept	12.64***	1.81	< 0.001	< 0.001		9.04	16.24
Average controllability	1.56	1.64	0.35	0.72	0.21	-1.71	4.83
Negative Affect	0.14**	0.04	0.002	0.008	0.70	0.05	0.23
Total brain volume	0.17	0.65	0.80	0.99	0.06	-1.12	1.45
In-scanner motion	-0.18	0.71	0.80	0.99	-0.06	-1.58	1.23
Random effects							
Intercept	0.72						
Residual	37.90						
Dorsal Attention A							
Fixed effects							
Intercept	12.60***	1.82	< 0.001	< 0.001		9.04	16.23
Average controllability	1.27	1.48	0.39	0.77	0.19	-1.67	4.21
Negative Affect	0.14**	0.04	0.002	0.008	0.71	0.05	0.23
Total brain volume	0.16	0.65	0.81	0.99	0.05	-1.13	1.45
In-scanner motion	-0.17	0.72	0.81	0.99	-0.05	-1.61	1.27
Random effects							
Intercept	0.92						
Residual	37.84						
Dorsal Attention B							
Fixed effects							
Intercept	12.66***	1.82	< 0.001	< 0.001		9.05	16.28
Average controllability	1.47	3.03	0.63	0.99	0.11	-4.56	7.50
Negative Affect	0.14**	0.04	0.002	0.008	0.70	0.05	0.23
Total brain volume	0.19	0.66	0.77	0.99	0.07	-1.11	1.50
In-scanner motion	-0.06	0.70	0.93	0.99	-0.02	-1.45	1.33
Random effects							
Intercept	0.74						
Residual	38.18						
Limbic A							
Fixed effects							
Intercept	12.62***	1.82	< 0.001	< 0.001		8.99	16.24
Average controllability	1.10	1.08	0.31	0.68	0.23	-1.05	3.25
Negative Affect	0.14**	0.04	0.002	0.008	0.71	0.05	0.23
Total brain volume	0.05	0.67	0.94	0.99	0.02	-1.28	1.38
In-scanner motion	-0.08	0.71	0.92	0.99	-0.02	-1.50	1.35
Random effects							
Intercept	1.07						
Residual	37.62						
Limbic B							
Fixed effects							
Intercept	12.66***	1.84	< 0.001	< 0.001		9.00	16.33
Average controllability	-0.19	1.08	0.86	0.99	-0.04	-2.34	1.97
Negative Affect	0.14**	0.05	0.003	0.008	0.69	0.05	0.23
Total brain volume	0.30	0.69	0.67	0.99	0.10	-1.08	1.68
In-scanner motion	-0.01	0.72	0.98	0.99	-0.004	-1.44	1.42
Random effects							

Intercept	0.91						
Residual	38.15						
Salience/Ventral Attention B							
Fixed effects							
Intercept	12.89***	1.83	< 0.001	< 0.001		9.24	16.54
Average controllability	1.06	1.38	0.44	0.85	0.17	-1.68	3.80
Negative Affect	0.14**	0.05	0.004	0.01	0.66	0.04	0.23
Total brain volume	0.05	0.70	0.94	0.99	0.02	-1.33	1.44
In-scanner motion	-0.07	0.69	0.92	0.99	-0.02	-1.45	1.31
Random effects							
Intercept	0.69						
Residual	38.06						
Somatomotor A							
Fixed effects							
Intercept	12.75***	1.82	< 0.001	< 0.001		9.13	16.38
Average controllability	-1.66	2.54	0.52	0.95	-0.14	-6.71	3.40
Negative Affect	0.14**	0.04	0.003	0.008	0.69	0.05	0.23
Total brain volume	0.18	0.65	0.79	0.99	0.06	-1.12	1.48
In-scanner motion	0.009	0.71	0.99	0.99	0.002	-1.41	1.43
Random effects							
Intercept	0.99						
Residual	37.93						
Somatomotor B							
Fixed effects							
Intercept	12.68***	1.81	< 0.001	< 0.001		9.07	16.28
Average controllability	1.11	1.73	0.52	0.95	0.14	-2.34	4.56
Negative Affect	0.14**	0.04	0.002	0.008	0.70	0.05	0.23
Total brain volume	0.15	0.66	0.82	0.99	0.05	-1.16	1.47
In-scanner motion	-0.03	0.69	0.96	0.99	-0.01	-1.41	1.34
Random effects							
Intercept	0.69						
Residual	38.13						
Temporal Parietal							
Fixed effects							
Intercept	12.73***	1.82	< 0.001	< 0.001		9.11	16.36
Average controllability	-0.56	1.25	0.65	0.99	-0.10	-3.04	1.92
Negative Affect	0.14**	0.04	0.003	0.008	0.69	0.05	0.23
Total brain volume	0.36	0.68	0.60	0.99	0.12	-1.00	1.72
In-scanner motion	-0.02	0.71	0.98	0.99	-0.007	-1.43	1.39
Random effects							
Intercept	0.93						
Residual	38.06						
Visual Central (Visual A)							
Fixed effects							
Intercept	12.64***	1.82	< 0.001	< 0.001		9.03	16.26
Average controllability	0.50	1.16	0.67	0.99	0.10	-1.81	2.81
Negative Affect	0.14**	0.04	0.002	0.008	0.70	0.04	0.23
Total brain volume	0.21	0.65	0.74	0.99	0.07	-1.08	1.51
In-scanner motion	-0.15	0.74	0.84	0.99	-0.04	-1.63	1.33
Random effects							
Intercept	0.70						

Residual	38.22						
Visual Peripheral (Visual B)							
Fixed effects							
Intercept	12.56***	1.81	< 0.001	< 0.001		8.96	16.17
Average controllability	1.11	1.12	0.32	0.68	0.22	-1.11	3.34
Negative Affect	0.14**	0.04	0.002	0.008	0.71	0.05	0.23
Total brain volume	0.16	0.65	0.81	0.99	0.05	-1.13	1.45
In-scanner motion	-0.25	0.72	0.73	0.99	-0.08	-1.69	1.19
Random effects							
Intercept	0.71						
Residual	37.87						

Note. 95 participants nested in 10 groups; ***$p < 0.001$; **$p \leq 0.01$. Total brain volume and in-scanner motion were sample-mean centered; average controllability was rank-based inverse normal transformed. p_{FDR} = adjusted p-values following Benjamini-Hochberg False Discovery Rate control (21).

Supplemental Table S7. Results of the multilevel model examining associations between average controllability of the cingulo-insular network with negative affect instability.

Effect	Estimate	Standard error	*p*	p_{FDR}	*d*	Confidence interval	
						Lower	Upper
Negative Affect Instability							
Fixed effects							
Intercept	239.32*	86.81	0.007	0.03		66.60	412.03
Average controllability	420.76	183.66	0.03	0.06	0.51	55.35	786.18
Negative Affect	7.14	2.17	0.001	0.008	0.73	2.82	11.45
Total brain volume	4.52	31.70	0.89	0.94	0.03	-58.56	67.60
In-scanner motion	24.38	30.78	0.43	0.65	0.18	-36.86	85.61
Random effects							
Intercept	4.72						
Residual	88913.34						

Note. 95 participants nested in 10 groups; ***$p < 0.001$; **$p \leq 0.01$; * $p \leq 0.05$. following false discovery rate control. Total brain volume and in-scanner motion were sample-mean centered; average controllability was rank-based inverse normal transformed; negative affect instability was measured using the mean successive squared difference of negative affect.

Supplemental Table S8. Results of the multilevel model examining associations between average controllability of the cingulo-insular network with negative affect inertia.

Effect	Estimate	Standard error	p	p_{FDR}	d	Confidence interval	
						Lower	Upper
Negative Affect Inertia							
Fixed effects							
Intercept	0.15***	0.04	< 0.001	< 0.001		0.07	0.22
Average controllability	0.18	0.14	0.21	0.64	0.28	-0.10	0.47
Total brain volume	-0.006	0.03	0.81	0.98	-0.05	-0.06	0.04
In-scanner motion	0.02	0.03	0.61	0.95	0.11	-0.05	0.09
Random effects							
Intercept	0.005						
Residual	0.06						

Note. 95 participants nested in 10 groups; ***$p < 0.001$; **$p \leq 0.01$ following false discovery rate control. Total brain volume and in-scanner motion were sample-mean centered; average controllability was rank-based inverse normal transformed; negative affect inertia was calculated using the intraindividual autocorrelation.

Supplemental Table S9. Correlations of network metrics.

Control A	1	2	3	4
1. Strength				
2. Average Controllability	.69**			
3. Clustering Coefficient	.11	-.15		
4. Betweenness Centrality	-.04	-.15	-.03	
5. Closeness Centrality	.35**	.61**	-.61**	-.17

Control B	1	2	3	4
1. Strength				
2. Average Controllability	.71**			
3. Clustering Coefficient	.13	-.13		
4. Betweenness Centrality	.04	-.13	-.25*	
5. Closeness Centrality	.54**	.77**	-.32**	-.07

Control C	1	2	3	4
1. Strength				
2. Average Controllability	.63**			
3. Clustering Coefficient	.88**	.50**		
4. Betweenness Centrality	-.06	.09	-.22*	
5. Closeness Centrality	-.70**	-.18	-.70**	.03

Default A	1	2	3	4
1. Strength				
2. Average Controllability	.56**			
3. Clustering Coefficient	.43**	-.14		
4. Betweenness Centrality	-.08	-.05	-.11	
5. Closeness Centrality	.08	.69**	-.45**	-.13

Default B	1	2	3	4
1. Strength				
2. Average Controllability	.75**			
3. Clustering Coefficient	.11	-.13		
4. Betweenness Centrality	-.01	.15	-.36**	
5. Closeness Centrality	.48**	.70**	-.33**	.13

Default C	1	2	3	4
1. Strength				
2. Average Controllability	.66**			
3. Clustering Coefficient	.59**	.14		
4. Betweenness Centrality	-.02	.09	-.24*	
5. Closeness Centrality	-.10	.36**	-.64**	.12

Dorsal Attention A	1	2	3	4
1. Strength				

2. Average Controllability	.74**			
3. Clustering Coefficient	.61**	.36**		
4. Betweenness Centrality	.19	.17	-.18	
5. Closeness Centrality	-.26*	.14	-.62**	.03

Dorsal Attention B	1	2	3	4
1. Strength				
2. Average Controllability	.54**			
3. Clustering Coefficient	.72**	.38**		
4. Betweenness Centrality	-.03	-.11	-.03	
5. Closeness Centrality	-.13	.13	-.57**	-.13

Limbic A	1	2	3	4
1. Strength				
2. Average Controllability	.55**			
3. Clustering Coefficient	.14	-.42**		
4. Betweenness Centrality	.16	.47**	-.51**	
5. Closeness Centrality	.19	.63**	-.67**	.43**

Limbic B	1	2	3	4
1. Strength				
2. Average Controllability	.75**			
3. Clustering Coefficient	.35**	.05		
4. Betweenness Centrality	.02	.02	-.31**	
5. Closeness Centrality	.46**	.75**	-.13	-.04

Salience/Ventral Attention A	1	2	3	4
1. Strength				
2. Average Controllability	.24*			
3. Clustering Coefficient	.69**	-.10		
4. Betweenness Centrality	-.20*	-.05	-.08	
5. Closeness Centrality	-.40**	.32**	-.74**	-.12

Salience/Ventral Attention B	1	2	3	4
1. Strength				
2. Average Controllability	.88**			
3. Clustering Coefficient	.36**	.23*		
4. Betweenness Centrality	.32**	.33**	-.25*	
5. Closeness Centrality	.71**	.80**	-.00	.28**

Somatomotor A	1	2	3	4
1. Strength				
2. Average Controllability	.63**			
3. Clustering Coefficient	.85**	.62**		
4. Betweenness Centrality	-.06	-.11	-.12	
5. Closeness Centrality	-.52**	-.51**	-.76**	.02

Somatomotor B	1	2	3	4
1. Strength				
2. Average Controllability	.56**			
3. Clustering Coefficient	.58**	.13		
4. Betweenness Centrality	.00	-.05	-.26*	
5. Closeness Centrality	.05	.40**	-.48**	.00

Temporal Parietal	1	2	3	4
1. Strength				
2. Average Controllability	.33**			
3. Clustering Coefficient	.50**	.06		
4. Betweenness Centrality	-.08	.19	-.22*	
5. Closeness Centrality	-.18	.44**	-.35**	.02

Visual Central (Visual A)	1	2	3	4
1. Strength				
2. Average Controllability	.70**			
3. Clustering Coefficient	.55**	.24*		
4. Betweenness Centrality	.45**	.36**	.05	
5. Closeness Centrality	-.12	.33**	-.55**	-.05

Visual Peripheral (Visual B)	1	2	3	4
1. Strength				
2. Average Controllability	.81**			
3. Clustering Coefficient	.76**	.48**		
4. Betweenness Centrality	-.18	-.01	-.26*	
5. Closeness Centrality	.01	.32**	-.46**	.09

Note. ** indicates $p < 0.01$. * indicates $p < 0.05$.

Supplemental Table S10. Correlations and descriptive statistics of emotion dynamics variables.

Variable	*M*	*SD*	1	2
1. Negative affect variability	17.88	6.44		
2. Negative affect instability	310.84	244.51	.81**	
3. Negative affect inertia	0.15	0.24	.17	-.08

Note. M and *SD* are used to represent mean and standard deviation, respectively. ** indicates $p < 0.01$.

Supplemental Figure S1. CONSORT flow diagram of study enrollment and retention across periods.

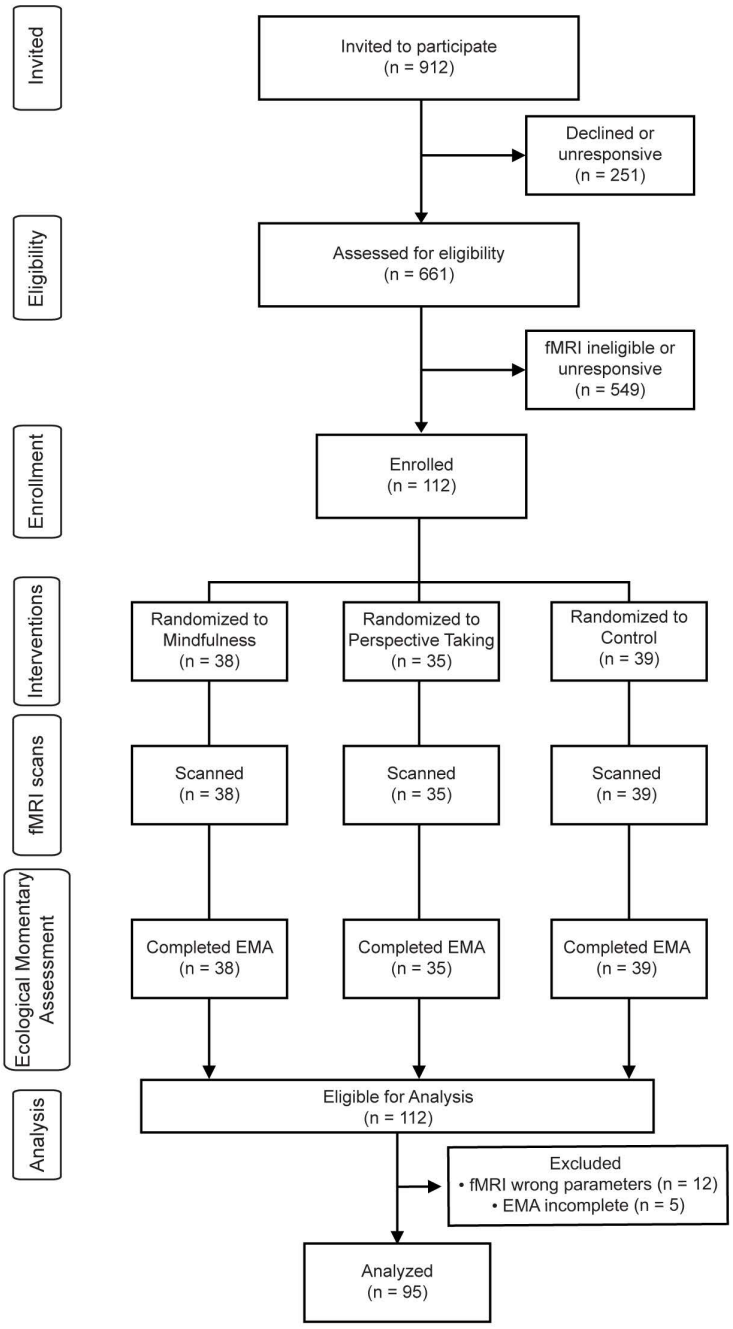

Supplemental Figure S2. Association between negative affect variability and presence of depressive symptoms. Greater negative affect variability relates to the presence of more depressive symptoms.

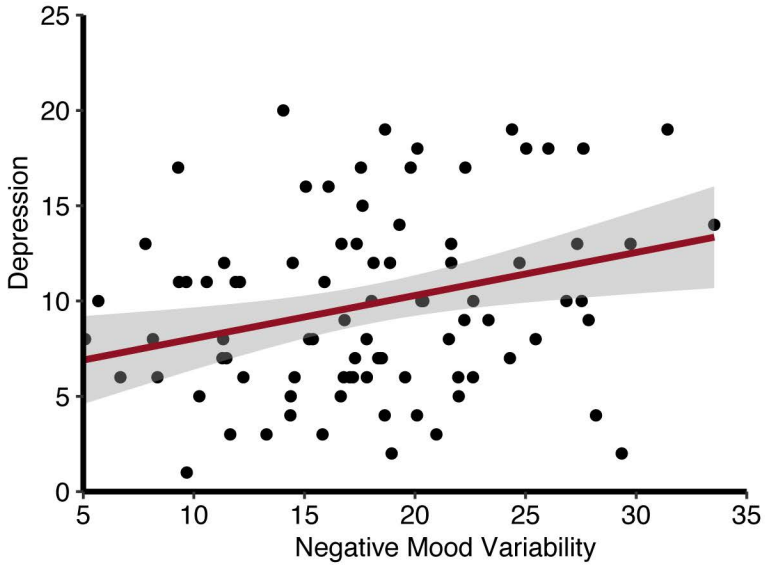

Supplemental References

1. Tustison NJ, Avants BB, Cook PA, Zheng Y, Egan A, Yushkevich PA, Gee JC (2010): N4ITK: improved N3 bias correction. *IEEE transactions on medical imaging* 29: 1310–1320.

2. Fonov VS, Evans AC, McKinstry RC, Almli CR, Collins DL (2009): Unbiased nonlinear average age-appropriate brain templates from birth to adulthood. *NeuroImage* S102.

3. Avants BB, Epstein CL, Grossman M, Gee JC (2008): Symmetric diffeomorphic image registration with cross-correlation: evaluating automated labeling of elderly and neurodegenerative brain. *Medical image analysis* 12: 26–41.

4. Zhang Y, Brady M, Smith S (2001): Segmentation of brain MR images through a hidden Markov random field model and the expectation-maximization algorithm. *IEEE transactions on medical imaging* 20: 45–57.

5. Veraart J, Novikov DS, Christiaens D, Ades-Aron B, Sijbers J, Fieremans E (2016): Denoising of diffusion MRI using random matrix theory. *Neuroimage* 142: 394–406.

6. Kellner E, Dhital B, Kiselev VG, Reisert M (2016): Gibbs-ringing artifact removal based on local subvoxel-shifts. *Magnetic resonance in medicine* 76: 1574–1581.

7. Andersson JL, Sotiropoulos SN (2016): An integrated approach to correction for off-resonance effects and subject movement in diffusion MR imaging. *Neuroimage* 125: 1063–1078.

8. Andersson JL, Skare S, Ashburner J (2003): How to correct susceptibility distortions in spin-echo echo-planar images: application to diffusion tensor imaging. *Neuroimage* 20: 870–888.

9. Power JD, Mitra A, Laumann TO, Snyder AZ, Schlaggar BL, Petersen SE (2014): Methods to detect, characterize, and remove motion artifact in resting state fMRI. *Neuroimage* 84: 320–341.

10. Abraham A, Pedregosa F, Eickenberg M, Gervais P, Mueller A, Kossaifi J, *et al.* (2014): Machine learning for neuroimaging with scikit-learn. *Frontiers in neuroinformatics* 8: 14.

11. Contributors D, Garyfallidis E, Brett M, Amirbekian BB, Rokem A, van der Walt S, *et al.* (2014): Dipy, a library for the analysis of diffusion MRI data. *Frontiers in Neuroinformatics* 8: 8.

12. Rubinov M, Sporns O (2010): Complex network measures of brain connectivity: uses and interpretations. *Neuroimage* 52: 1059–1069.

13. Liu J, Li M, Pan Y, Lan W, Zheng R, Wu F-X, Wang J (2017): Complex Brain Network Analysis and Its Applications to Brain Disorders: A Survey. *Complexity* 2017: e8362741.

14. Perez C, Germon R (2016): Graph creation and analysis for linking actors: application to social data. *Automating Open Source Intelligence*. Elsevier, pp 103–129.

15. Golbeck J (2013): Chapter 3 - Network Structure and Measures. In: Golbeck J, editor. *Analyzing the Social Web*. Boston: Morgan Kaufmann, pp 25–44.

16. Jahng S, Wood PK, Trull TJ (2008): Analysis of affective instability in ecological momentary assessment: Indices using successive difference and group comparison via multilevel modeling. *Psychological Methods* 13: 354–375.

17. Wang L (Peggy), Hamaker E, Bergeman CS (2012): Investigating inter-individual differences in short-term intra-individual variability. *Psychological Methods* 17: 567–581.

18. Von Neumann J, Kent RH, Bellinson HR, Hart BI (1941): The mean square successive difference. *The Annals of Mathematical Statistics* 12: 153–162.

19. Sperry SH, Walsh MA, Kwapil TR (2020): Emotion dynamics concurrently and prospectively predict mood psychopathology. *Journal of affective disorders* 261: 67–75.

20. Kuppens P, Allen NB, Sheeber LB (2010): Emotional inertia and psychological maladjustment. *Psychological science* 21: 984–991.

21. Benjamini Y, Hochberg Y (1995): Controlling the false discovery rate: a practical and powerful approach to multiple testing. *Journal of the Royal statistical society: series B (Methodological)* 57: 289–300.